# Polarization-maintaining photonic-crystal-fiber-based all-optical polarimetric torsion sensor

H. Y. Fu,[1] Sunil K. Khijwania,[2,*] H. Y. Tam,[1] P. K. A. Wai,[1] and C. Lu[1]

[1]Photonics Research Centre, The Hong Kong Polytechnic University, Kowloon, Hong Kong

[2]Department of Physics, Indian Institute of Technology, Guwahati, India

*Corresponding author: skhijwania@iitg.ernet.in

An application of a polarization-maintaining photonic crystal fiber (PM-PCF) for torsion sensing is proposed and experimentally demonstrated. The response of the sensor is theoretically validated using the Jones matrix. High normalized sensitivity of ~0.014/° was measured within a linear twist angle range from 30° to 70°. The sensor response was observed to be highly repeatable over a 90° twist in both the clockwise and counterclockwise directions. The proposed sensor exhibits reduced temperature sensitivity due to the low thermal coefficient of PM-PCF, making it an ideal candidate for torsion sensing.   © 2010 Optical Society of America

 *OCIS codes:*    060.2370, 060.3735.

## 1. Introduction

The unique characteristics of photonic crystal fiber (PCF), such as manipulation of fiber characteristics with careful design of air-hole parameters, endlessly single-mode guidance, and large signal–sample interaction length, have attracted much research interest in recent years. In particular, sensing applications using PCFs have also been widely explored. However, most research efforts mainly exploit PCF characteristics to realize gas/liquid sensors with guided-wave/evanescent-wave interaction [1–5]. It has been established that PCF-based optical fiber sensors offer extraordinary sensitivity for gas/liquid monitoring. Recently, polarization-maintaining PCFs (PM-PCFs) have been studied for pressure/strain sensing [6–8]. PM-PCFs offer additional advantages owing to their high birefringence and low thermal sensitivity [9,10]. However, to the best of the authors' knowledge, PCFs/PM-PCFs are rarely exploited for torsion monitoring. Torsion is an important parameter for structural health monitoring and many other kinds of engineering applications. All-optical torsion sensors, based on fiber Bragg gratings (FBGs), long period gratings (LPGs), and high birefringence fibers, have been reported in the literature [11–14]. In the FBG-based torsion sensor [11], an FBG was bonded onto the surface of a solid copper shaft. Applying pure torsion to the shaft resulted in an induced strain along the surface and, hence, along the glued FBG. This strain-induced Bragg wavelength shift was measured to sense the applied torsion with limited twist angle range determined by the shaft. In Ref. [12], a torsion sensor based on a 16 mm long HF-etched corrugated LPG was reported with a twist sensitivity of $0.036 \, \mathrm{nm}/(\mathrm{rad} \, \mathrm{m}^{-1})$. In Ref. [13], researchers demonstrated resonant wavelength dependence of twist angle and direction in $CO_2$ induced LPG with twist sensitivity of up to $0.032 \, \mathrm{nm}/(\mathrm{rad} \, \mathrm{m}^{-1})$. In another scheme [14], a torsion sensor based on an FBG written in high birefringence fiber was proposed with a twist angle resolution of about 0.3°. All the reported torsion sensors [11–14] are based on the doped fibers that exhibit relatively large temperature-dependent cross talk. Typical temperature coefficients of FBGs written in standard fibers and PM fibers are $10 \, \mathrm{pm}/°\mathrm{C}$ and $14 \, \mathrm{pm}/°\mathrm{C}$ [15], respectively, and that in LPGs is generally much larger. In contrast, PCFs are made

entirely of fused silica, which has a low thermal expansion coefficient. Consequently, fiber optic sensors based on PCFs are less temperature dependent. Recently, preliminary information for the possible application of PM-PCF for torsion monitoring was reported by the authors of this paper [16].

In this paper, we report for the first time, to the best of our knowledge, a detailed experimental demonstration along with an exhaustive theoretical analysis of an optical fiber polarimetric torsion sensor based on PM-PCF. A simplified theoretical analysis is also given to explain the operation principle of the proposed torsion sensor. The twist angle of the PM-PCF-based torsion sensor was measured with polarimetric detection. Normalized sensitivity as high as $\sim 0.014/°$ was measured within the linear twist angle range from 30° to 70°. The sensor response was observed to be highly reversible and repeatable over 90° twist in both the clockwise (CW) and counterclockwise (CCW) directions. Owing to the low thermal coefficient of PM-PCF, our proposed torsion sensor eliminates the requirement of temperature compensation when deployed in a harsh environment where temperature fluctuation is inevitable. High birefringence of the PM-PCF ensures that the torsion sensor will be compact, releasing the limitation of the torsion gauge length.

## 2. Experimental Setup and Operating Principle

Figure 1 illustrates the experimental setup of the proposed PM-PCF-based torsion sensor. The light source used in this experiment was a tunable semiconductor laser (Santec, Model TSL-210) operating at 1550 nm. The polarization extinction ratio of this light source was higher than 40 dB. A polarization controller (OFR) was used to adjust the polarization state of the light launched into the PM-PCF. The PM-PCF (PM-1550-01, produced by BlazePhotonics) had a beat length of <4 mm at 1550 nm and a polarization extinction ratio of >30 dB over 100 m. The scanning electron micrograph image of the transverse cross section of the PM-PCF is shown in the inset of Fig. 1. Mode field diameters for the two orthogonal polarizations were 3.6 and 3.1 $\mu$m, respectively. The total loss of the two splicing points was $\sim 4$ dB and was achieved by repeated arc discharges applied over the splicing points to collapse the air
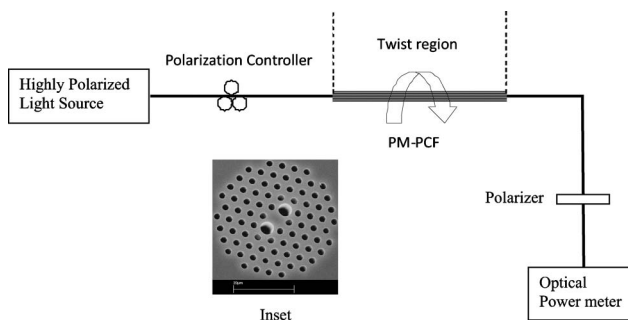
holes of the small-core PM-PCF [17]. The length of the PM-PCF used in this experiment was $\sim 15$ cm.

The optical sensing system was set up on an optical table to ensure stability. Initially, one end of the straight and horizontal section of the PM-PCF was fixed on a mount and the other end on a twist stage without any prestraining or pretwisting. The twist stage was capable of applying the required twist with the twist angle measurement provision. Owing to the limitation of setup, the smallest twist that could be applied in the present study was 1°. Polarimetric detection of the output light signal was achieved with a linear polarizer (Optics for Research OFR, Thorlabs) together with a powermeter (Ilxlightwave, FSM-8210). Initially, the polarization state of the polarization controller was adjusted to obtain maximum power at the output. Maximum output power can be achieved only when the polarization state of the output light is parallel to the pass axis of the linear polarizer. Hence, we adjusted the polarization controller and the linear polarizer both to get the maximum output power at the beginning. With the PM-PCF under twist, the optical output power was observed to vary as a function of the twist angle.

Figure 2 shows the coordinate of the principal axis for the fiber optic torsion sensing system. $\theta$ is the angle made by the pass axis of the linear polarizer with the $x$ axis, $\beta$ is the principal axis angle of the PM-PCF input end with respect to the $x$ axis, and $\alpha$ is the twist angle of the PM-PCF. Considering the polarization state of the light during propagation, the optical system can be described as [18]

$$
\begin{bmatrix} E_x^{\text{out}} \\ E_y^{\text{out}} \end{bmatrix} = [\text{Polarizer}(\theta)][\text{Rotation}(-\beta)][\text{Rotation}(-\alpha)]
$$
$$
\times [M(\alpha, \delta)][\text{Rotation}(\beta)] \begin{bmatrix} E_x^{\text{in}} \\ 0 \end{bmatrix}, \qquad (1)
$$

where $E_x^{\text{in}}$ is the amplitude of the input highly polarized light, and $E_x^{\text{out}}$ and $E_y^{\text{out}}$ are the amplitudes of the two orthogonal polarized lights at the output end. The Jones matrix of the linear polarizer is given as



Fig. 1. Schematic diagram of the proposed PM-PCF-based fiber optic polarimetric torsion sensor.
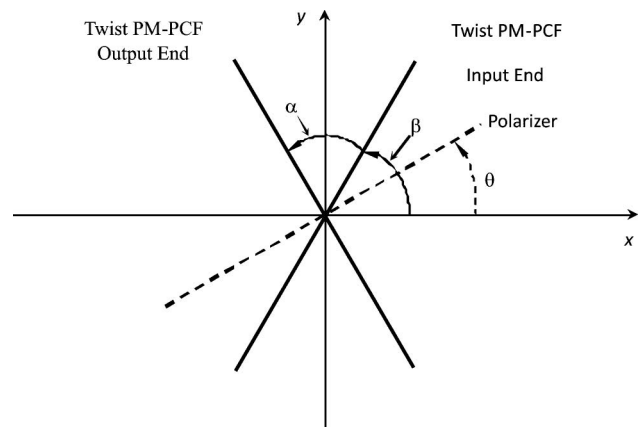


Fig. 2. Coordinate of the principal axis for the fiber optic torsion sensing system.

$$[\text{Polarizer}(\theta)] = \begin{bmatrix} \cos^2(\theta) & \cos(\theta)\sin(\theta) \\ \sin(\theta)\cos(\theta) & \sin^2(\theta) \end{bmatrix}. \quad (2)$$

The Jones matrix for the coordinate rotation with angle $\sigma$ is given as

$$[\text{Rotation}(\sigma)] = \begin{bmatrix} \cos(\sigma) & \sin(\sigma) \\ -\sin(\sigma) & \cos(\sigma) \end{bmatrix}, \quad (3)$$

and the Jones matrix of the twisted PM-PCF is given as

$$[M(\alpha,\delta)] = \begin{bmatrix} \cos\gamma - (i\cdot\delta\cdot\sin\gamma)/\gamma & \alpha\cdot\sin\gamma/\gamma \\ -\alpha\cdot\sin\gamma/\gamma & \cos\gamma + (i\cdot\delta\cdot\sin\gamma)/\gamma \end{bmatrix}, \quad (4)$$

where $\gamma = (\alpha^2 + \delta^2)^{1/2}$, $\delta = \pi\cdot l_T\cdot(n_x - n_y)/\lambda$, and $l_T$ is the length of PM-PCF. The phase retardation angle of the PM-PCF is $2\delta$. The output power of polarimetric detection thus can be obtained as

$$I = \begin{bmatrix} E_x^{\text{out}} & E_y^{\text{out}} \end{bmatrix} \cdot \begin{bmatrix} E_x^{\text{out}} \\ E_y^{\text{out}} \end{bmatrix}^*. \quad (5)$$

The PM-PCF used in the present experiment had a high birefringence with a beat length of less than 4 mm. Further, the length of the PM-PCF used in the experiment was ~15 cm. Hence, $\alpha \ll 2\delta$. Under this condition, the twisted PM-PCF acts as an optical rotator and the system becomes insensitive to the gauge length [14]. The arrangement in which the polarization controller and the linear polarizer both were adjusted to achieve a maximum output power at the beginning can be well described by assuming $\beta = 90°$ and $\theta = 0°$. This leads to the output optical intensity approximately as

$$I = \cos^2\alpha\cdot|E_x^{\text{in}}|^2, \quad (6)$$

enabling us to calculate the output intensities for any different combinations of $\theta$ and $\beta$. Figure 3 shows the calculated output intensity as a function of twist angle for different values of $\beta$ under a simplified situation where the pass axis of the linear polarizer is considered as the $x$ axis itself, thus restricting $\theta = 0°$. $\beta$ is varied in a step of 15° over the full range of 90°. As is evident from Fig. 3, the maximum dynamic range for the output intensity is achieved only when $\beta = 0°$ or 90° (solid curve).

## 3. Results and Discussion

Figure 4 shows the measured output power as a function of twist angle applied to the PM-PCF. As can be observed, the output power is highly sensitive to the applied twist with a variation of more than 12 dB when the twist angle was varied in the range of $\pm\pi/2$. In addition, the power variation was highly symmetric with respect to the zero twist (unperturbed) position. The same figure shows the sensor response when the PM-PCF was twisted from $-\pi/2$
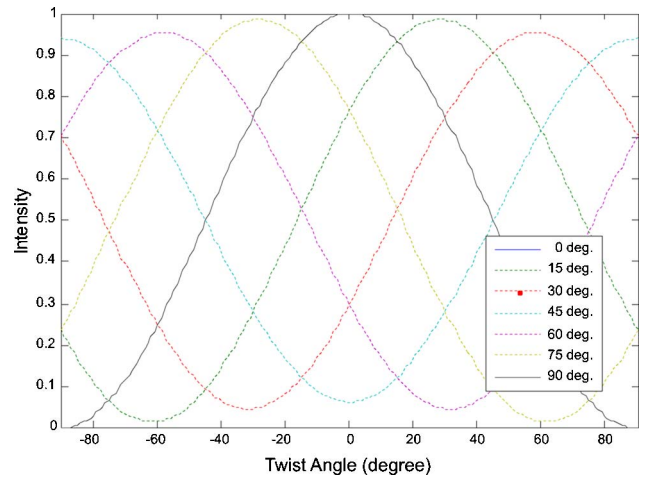


Fig. 3. (Color online) Output intensity of the torsion sensor under the $\theta = 0°$ condition, where $\beta$ is varied from 0° to 90° in steps of 15°.

to $\pi/2$ (CW or forward twist) (blue diamonds) and then from $\pi/2$ to $-\pi/2$ (CCW or reverse twist) (pink circles). These results show a complete reversible nature of the proposed torsion sensor. As can be seen, the twist sensitivity varies with the twist angle. For a small twist angle, the power level follows a slowly decreasing smooth curve, while at larger twist angles, the power level falls sharply. To have a deeper analysis, the sensor response was theoretically simulated and the consistency between experimental and theoretical results was then investigated. Figure 5 illustrates theoretically simulated (as discussed in Section 2) as well as experimental observed normalized output intensities against the twist angles. Sensor response matches qualitatively well with that of the theoretically simulated one for the entire range of applied twist. A high degree of quantitative agreement was observed when the applied twist to the PM-PCF was small (~20°). However, for higher twist angles, experimentally observed intensities were little higher in comparison to the theoretically predicted intensities. This is because of the received optical power at other polarization states, which is not perfectly filtered out through the linear polarizer. This also explains the fact that the experimentally observed power did not go to zero when the applied
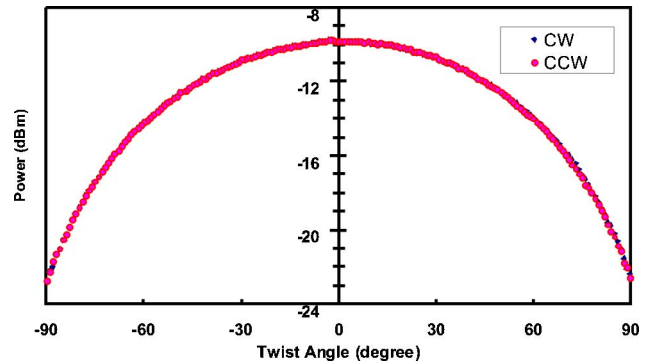


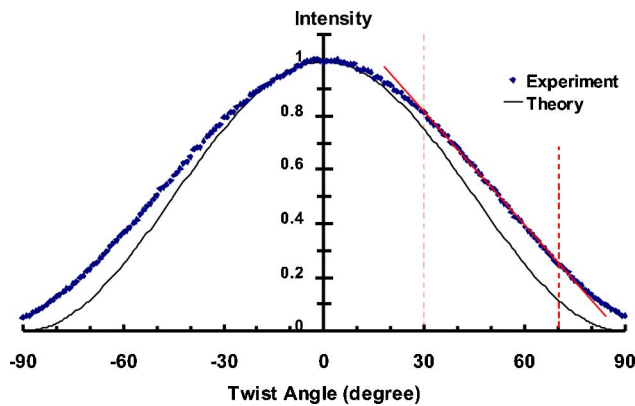Fig. 4. (Color online) Measured output power versus twist angle of a PM-PCF.

Fig. 5. (Color online) Normalized experimental and theoretical (with $\beta = 90°$ and $\theta = 0°$) intensities versus twist angle.

twist was close to $\pm 90°$. From $30°$ to $70°$, the power decreases with good linearity and the calculated slope (normalized sensitivity) is $\sim 0.014/°$. This linear region is of extreme importance when designing a real sensing device for practical applications. Further, the sensing fiber element can be pretwisted to this range in order to suitably resolve a twist that is even less than $30°$. As an example, torsion sensor response was theoretically simulated for a pretwist angle of $\pm 45°$ for the PM-PCF sensor. Figure 6 shows the theoretical prediction for these two pretwist angles. As can be observed from the sensor response in Fig. 6, an approximately linear region is achieved at zero twist angle, which validates our previous statement. Similarly, one can obtain a linear torsion sensing response over a large torsion range as per the need of an actual field application by suitably changing the pretwist angle.

The effect of an ambient temperature on the sensor response is a critical issue while designing a sensor system for field applications. Hence, the effects of ambient temperature fluctuations on the sensor performance were also investigated. For this, the sensing twisted PM-PCF was placed in a temperature controlled container, and the temperature with-
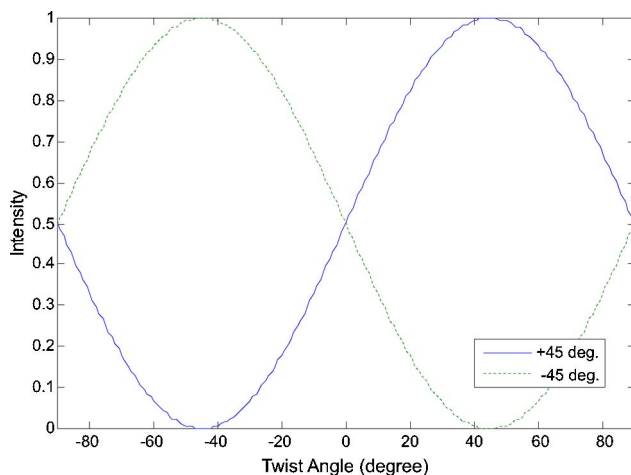


Fig. 6. (Color online) Output intensity of the torsion sensor with a pretwist angle of $+45°$ (solid curve) and $-45°$ (dashed curve).
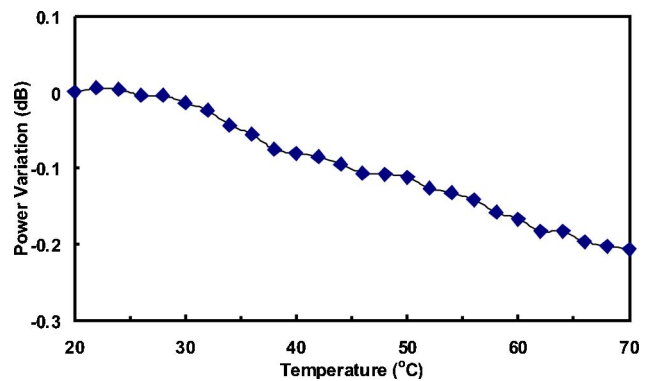


Fig. 7. Thermal response of the torsion sensing system.

in the container was varied from 20 °C to 70 °C. Figure 7 shows a typical sensor response under temperature variations. As can be observed, the power variation is only 0.2 dB against a temperature variation of 50 °C. This shows that the temperature sensitivity of the proposed sensor is negligibly small. Thus, if the proposed sensor is applied to an environment where temperature variation is not very large, the need for temperature compensation schemes can be completely eliminated.

## 4. Conclusion

An all-optical fiber torsion sensor employing a PM-PCF as a sensing element is experimentally demonstrated and analyzed theoretically for the first time, to the best of authors' knowledge. A very high sensitivity of the order of $\sim 0.014/°$ is experimentally achieved within the linear twist range (from $30°$ to $70°$). The sensor response is observed to be highly reversible and repeatable within the applied twist range of $\pm\pi/2$ in both the CW and CCW directions. Further, a simplified theoretical analysis of the torsion sensor is also carried out. Experimental results for the sensor response match well with the theoretically simulated one. Compared to the conventional fiber optical torsion sensors, the proposed sensor exhibits reduced temperature sensitivity, eliminating the temperature compensation requirements if the temperature variation is not very large. In addition, this sensor is simple to design, compact in size, easy to manufacture, and highly sensitivity to the applied twist. This makes it an ideal candidate for torsion sensing for real field applications.

## References

1. T. M. Monro, D. J. Richardson, and P. J. Bennett, "Developing holey fibres for evanescent field devices," Electron. Lett. **35**, 1188–1189 (1999).
2. Y. L. Hoo, W. Jin, C. Shi, H. L. Ho, D. N. Wang, and S. C. Ruan, "Design and modeling of a photonic crystal fiber gas sensor," Appl. Opt. **42**, 3509–3515 (2003).

3. J. M. Fini, "Microstructure fibres for optical sensing in gases and liquids," Meas. Sci. Technol. **15**, 1120–1128 (2004).

4. J. B. Jensen, L. H. Pedersen, P. E. Hoiby, L. B. Nielsen, T. P. Hansen, J. R. Folkenberg, J. Riishede, D. Noordegraaf, K. Nielsen, A. Carlsen, and A. Bjarklev, "Photonic crystal fiber based evanescent-wave sensor for detection of biomolecules in aqueous solutions," Opt. Lett. **29**, 1974–1976 (2004).

5. C. M. B. Cordeiro, E. M. dos Santos, C. H. Brito Cruz, C. J. de Matos, and D. S. Ferreira, "Lateral access to the holes of photonic crystal fibers—selective filling and sensing applications," Opt. Express **14**, 8403–8412 (2006).

6. H. Y. Fu, H. Y. Tam, L.-Y. Shao, X. Dong, P. K. A. Wai, C. Lu, and S. K. Khijwania, "Pressure sensor realized with polarization-maintaining photonic crystal fiber-based Sagnac interferometer," Appl. Opt. **47**, 2835–2839 (2008).

7. H. K. Gahir and D. Khanna, "Design and development of a temperature-compensated fiber optic polarimetric pressure sensor based on photonic crystal fiber at 1550 nm," Appl. Opt. **46**, 1184–1189 (2007).

8. X. Dong, H. Y. Tam, and P. Shum, "Temperature-insensitive strain sensor with polarization-maintaining photonic crystal fiber based Sagnac interferometer," Appl. Phys. Lett. **90**, 151113 (2007).

9. K. Suzuki, H. Kubota, S. Kawanishi, M. Tanaka, and M. Fujita, "Optical properties of a low-loss polarization-maintaining photonic crystal fiber," Opt. Express **9**, 676–680 (2001).

10. D.-H. Kim and J. U. Kang, "Sagnac loop interferometer based on polarization maintaining photonic crystal fiber with reduced temperature sensitivity," Opt. Express **12**, 4490–4495 (2004).

11. X. G. Tian and X. M. Tao, "Torsion measurement using fiber Bragg grating sensors," Exp. Mech. **41**, 248–253 (2001).

12. L. A. Wang, C. Y. Lin, and G. W. Chern, "A torsion sensor made of a corrugated long period fibre grating," Meas. Sci. Technol. **12**, 793–799 (2001).

13. Y. P. Wang, J. P. Chen, and Y. J. Rao, "Torsion characteristics of long-period fiber gratings induced by high-frequency $CO_2$ laser pulses," J. Opt. Soc. Am. B **22**, 1167–1172 (2005).

14. Y. L. Lo, B. R. Chue, and S. H. Xu, "Fiber torsion sensor demodulated by a high-birefringence fiber Bragg grating," Opt. Commun. **230**, 287–295 (2004).

15. D. Liu, N. Q. Ngo, S. C. Tjin, and X. Dong, "A dual-wavelength fiber laser sensor system for measurement of temperature and strain," IEEE Photonics Technol. Lett. **19**, 1148–1150 (2007).

16. H. Y. Fu, S. K. Khijwania, H. Y. Au, X. Dong, H. Y. Tam, P. K. A. Wai, and C. Lu, "Novel fiber optic polarimetric torsion sensor based on polarization-maintaining photonic crystal fiber," Proc. SPIE **7004**, 7004-158 (2008).

17. L. Xiao, W. Jin, and M. S. Demokan, "Fusion splicing small-core photonic crystal fibers and single-mode fibers by repeated arc discharges," Opt. Lett. **32**, 115–117 (2007).

18. S. Huang and Z. Lin, "Measuring the birefringence of single-mode fibers with short beat length or nonuniformity: a new method," Appl. Opt. **24**, 2355–2361 (1985).